Computers and Geotechnics 108 (2019) 244–256

Contents lists available at ScienceDirect

Computers and Geotechnics

journal homepage: www.elsevier.com/locate/compgeo

Research Paper

A modified valley shape factor for the estimation of rockfill dam settlement

Raksiri Sukkarak[a], Pornkasem Jongpradist[a,*], Pornthap Pramthawee[b]

[a] Civil Engineering Department, Faculty of Engineering, King Mongkut's University of Technology Thonburi, Thung Khru, Bangkok, Thailand
[b] Department of Public Works and Town & Country Planning, Phrayathai, Bangkok, Thailand

ARTICLE INFO

Keywords:
Modified valley shape factor
Rockfill dam
Valley shape
Finite element analyses
Dam settlement behavior

ABSTRACT

This paper presents a series of finite element analyses aimed at investigating the influence of dam geometry, which in turn depends on the valley shape, on the settlement behavior of rockfill dams. The validity of the analysis method is verified with the well-instrumented case. All computed results show that the dam geometry, especially in narrow canyons, plays an important role in the dam settlement behavior. The evidence is interpreted through a modified valley shape factor S_β proposed in this study taking into account the abutment slope, which provides a more rational approach to gain insight into the effect of valley shape.

1. Introduction

Due to numerous advantages over their counterparts, more rockfill dams are popularly constructed in several parts of the globe. The deformation of rockfill is the main concern with this dam type. Large deformation inevitably causes abnormal behavior, which may cause potential havoc to the dam, such as in the concrete face slab type, cracks in the concrete face slab [1] and longitudinal cracks in the connection zone between different materials [2,3]. The deformation of the cushion layer often causes excessive stress in the concrete face slab component [4]. To mitigate these problems, it is important to improve the predictive ability regarding dam deformation behavior in the design stage.

It is well recognized that the adaptability to any topography is the main advantage of this dam type and that such a dam can be established in any canyon conditions. The dam shapes are diverse, mainly depending on the riverbed width, abutment and dam slopes. Due to the three-dimensional (3D) nature of rockfill dams, [5] recognized the importance of the effects of arching in narrow valleys. The factor that mainly contributes to the dam deformation is not only the material design/property, but also the dam geometry, and the dam valley shape has become an important issue in dam engineering practice [6–13].

For other dam types, a few valley shape factors have been suggested to take into account the dam geometry. They have been developed based on the ratio of the dam crest length between the valley abutments and dam height. The variation of abutment slope angle has been included in the later development by Kirn and Sarkaria [14] and Thomas [15]. Besides, the concept of valley shape as V, U and Y shapes is introduced to characterize the dam volume, safety factor and arch effect of compacted rockfill dams by Znamensky [16]. Among the available factors, the commonly used valley shape factor in the current practice is one introduced by Pinto and Marquez [17]; $A/H^2(SF)$, where A = concrete face slab area and H = dam height. They proposed an approximate estimation based on historical dam data for the dam deformation modulus during the construction ($E_{rc} = \gamma H d/\delta_s$) with the SF. Here, E_{rc} is in MPa; γ is unit weight of the rockfill in kN/m^3; δ_s is settlement of layer of thickness d due to the construction of the dam to a thickness H above that layer. The predictive method shows that the influence of valley shape is dominant when the SF is less than 3.5, resulting in a higher dam deformation modulus during construction. This influence appears to be the result of arching across the canyon and stress transfer of load into the abutments. Guidici et al. [18] and Kim and Kim [19] reported that a higher deformation modulus typically occurs in narrower valley conditions for well-compacted rockfill dams based on data obtained from the Hydro Electric Commission (Tasmania) and 30 cases of measured data from 7 countries. Pinto [20] presented a correlation between $E_{rc}/\gamma H$ and A/H^2 to emphasize the importance of the 3D effect on the concrete face slab. Consequently, he also proposed the safe line to identify the safe zone expressed by the following equation:

$$E_{rc}/\gamma H = 120 - 20A/H^2 \quad (1)$$

In addition, Johannesson [21] proposed a relationship between A/H^2 and δ/H to highlight the effect of valley shape on observed dam deformation ratio, as indicated by the black solid line in Fig. 1 based on his collected data (solid black diamond symbols). All settlements are

* Corresponding author at: Civil Engineering Department, Faculty of Engineering, King Mongkut's University of Technology Thonburi, 126 Pracha Uthit Rd., Bang Mod, Thung Khru, Bangkok 10140, Thailand.
E-mail address: pornkasem.jon@kmutt.ac.th (P. Jongpradist).

https://doi.org/10.1016/j.compgeo.2019.01.001
Received 17 September 2018; Received in revised form 19 December 2018; Accepted 1 January 2019
0266-352X/ © 2019 Elsevier Ltd. All rights reserved.

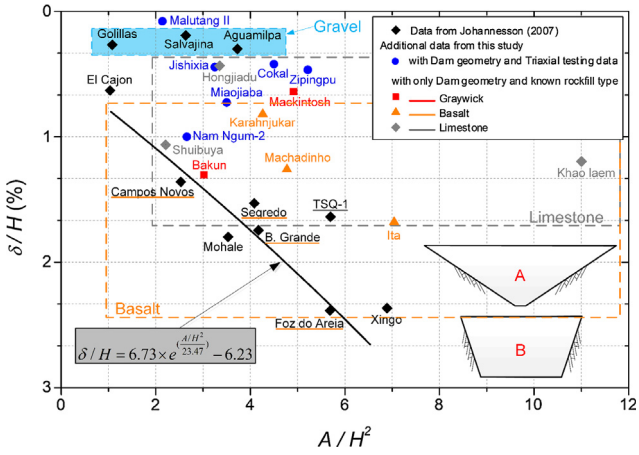

Fig. 1. Percentage settlement with the valley shape (modified from Johannesson [21]).

the maximum values measured in the dam body obtained at the end of construction stage. The suggested line can be best fitted by the exponential equation as also shown in the figure. In the figure, additional dam data from more recent constructions collected in this study are also included. The blue[1] circle symbols represent a total of 6 well-documented dams, including the typical layout of the dam for both transverse and longitudinal cross sections, dam instrument data and triaxial test results for rockfills. For the other data, the triaxial test data are not available in the literature, and information only on dam geometry could be found. The new data cover a wider range of A/H^2 and various kinds of rockfills and dam geometries. The figure clearly shows that the dam settlement ratio generally becomes larger with increasing A/H^2 (open valley), although some scattering can be noticed. The new data are generally below the suggested line by Johannesson [21] when the conditions are in the range of a wide valley. It is interesting to note that different settlement ratios can be observed for the dams whose A/H^2 values are in the same range (i.e., Nam Ngum-2, Jishixia and Miaojiaba). As illustrated by dams A and B (Fig. 1), the influence of valley shape conditions would be different with dissimilar dam geometry/abutment slopes. However, the values of A/H^2 for both conditions were the same. With further investigation, it is seen that they all possess different shapes, particularly the abutment slope (or valley shape – see detailed investigation in Section 4.2). This result implies that the parameter A/H^2 may be no longer sufficient to represent the valley effect and to cover a wide range of valley shapes.

Furthermore, as shown in Fig. 1, the type of rockfill material is apparently one of the important factors in dam settlement. This factor highlights the significance of the developments in construction technology, as the dams built during the past two decades have outstanding records with smaller settlement values, i.e., Zipingpu (2006), Jishixia (2007) and Malutang II (2009). The observation in the present study is similar to that revealed by Guidici et al. [18]. The variations in rock strength and stress levels are attributed to the scattering of the data. The reduction in dam settlement is partly due to the development of a compaction technique that increases the stiffness (E) of rockfill materials. Table 1 summarizes the concrete face rockfill dam (CFRD) data used in this study, which were mainly obtained from Cruz et al. [22].

For other dam types (i.e., concrete gravity, arch dams), the effect of dam shape has been widely explored [30–35]. Comparatively little work has been done and rarely mentioned on the effect of dam geometry on the deformation behavior of rockfill dams, even though more than 70% of dams worldwide are earth and rockfill dams. In previous works, Guidici et al. [18] conducted a series of 2D finite element analyses of an idealized rockfill embankment based on the elastic parameters. The study revealed the influence of the dam abutment slope and river width on vertical stress transmitted to deeper levels. The effect of dam valley conditions on the induced stresses in a concrete face slab has been explored in recent work using 3D-FEM [13]. However, very limited research has been performed with respect to the combined influences of dam geometry, especially the abutment slope β and dam slope α (see Fig. 2(a) and (b)), on dam settlement. Note that the dam slope is denoted by d values (i.e., 1.2, 1.4) instead of an angle in this study.

During the past two decades, large contributions to the development of dam deformation analyses have been carried out using the finite element (FE) method in the following categories: dam deformation during construction and impounding processes (e.g., [13,19,26,29,36–39]), creep analysis [37,40,41], back-parameter analysis (e.g., [26,42]) and development of the constitutive models (e.g., [43,44]). Although finite element analyses are commonly performed and provide reliable predictions for rockfill dam deformation under various conditions, estimation of rockfill dam settlement by some empirical methods is still necessary in engineering practice, especially for preliminary design [4,6,45]. As previously mentioned, despite A/H^2 providing a practical and convenient way for dam engineers to quantify the effect of dam valley shape conditions on dams constructed in the past, this ratio seems to be insufficient for a wide range of dam shapes. Moreover, with recently increasing of the dam height, the dam settlement behavior is also influenced by the magnitude of dam height [16] and several empirical relationships to estimate dam settlements have been proposed for the construction stage [19], first impoundment [17,19] and long-term settlement [7,8,46–49] on the case-by-case basis.

In this study, the effect of dam geometry on dam deformation behavior is investigated. The analysis method used is validated by a case study on the Nam Ngum 2 CFR dam. To verify our hypothesis, a preliminary investigation is presented first in which A/H^2 is evaluated by four FE analysis cases. Subsequently, a parametric study is carried out to analyze the influences of the dam geometry (abutment slope, dam slope and dam height) and the stiffness of rockfill material on the settlement behavior of rockfill dams. The valley shape factor is thus modified by taking into account the abutment slope. Based on the modified valley shape factor, a method for estimating dam settlement is suggested. The predictability has been proven on the basis of the parametric FE analysis results and dam data from case histories. The outcome of the investigation can be useful for dam designers and can provide insight into the effects of the dam geometry and the stiffness of rockfill material on dam settlement behavior.

2. Preliminary investigation

Although previous studies have provided valuable information for understanding the effects of valley shape conditions, it is difficult to draw comprehensive conclusions on dam deformation using only real dam data. Therefore, further investigation based on the parametric FE method is required. To demonstrate the dam behavior under various topographic situations (which in turn reflect the valley shape effect), four analyses were carried out. All four cases are carefully designed to possess the same face slab area (A) and dam height (H) but different dam topographic situations. For the longitudinal cross section, the different topographic situations can be visualized as different abutment slopes (β), crest lengths (L_c) and river widths (L_r), as shown in Fig. 2. Note that β is measured from the vertical axis; as a result, a smaller β indicates a steeper abutment slope. The details of 3D FE analyses can be found in the next section, and only the computed results are presented in this section. Fig. 3 shows the δ/H values plotted against L_r for the four analysis cases. The dam settlement (δ) was obtained at the deepest dam cross section at the mid-length in the longitudinal direction. In the figure, it is obvious that the settlement of dams with steeper abutment

[1] For interpretation of color in Figs. 1, 6, 10, 11, 14 and 17, the reader is referred to the web version of this article.

Table 1
Select details and dam characteristic of CFRDs used in this study.

Name	Country	Year	H (m)	δ (m)	L_c (m)	SF (A/H^2)	β_{avg} (°)	d		Rockfill type	E_{50}^{ref} (MPa)
								US	DS		
Golillas[a]	Columbia	1978	125	0.39	108	1.07	15	1.6	1.6	Gravel	NIA
El Cajon[a]	Mexico	2007	188	1.19	550	3.21	NIA	1.4	1.4	Ignimbrite	NIA
Salvajina[a]	Columbia	1983	148	0.28	362	2.62	NIA	1.4	1.3	Gravel/Siltstone	NIA
Campos Novos[a]	Brazil	2006	202	2.75	592	2.52	40	1.4	1.3	Basalt	NIA
Aguamilpa[a]	Mexico	1993	187	0.56	660	3.72	NIA	1.5	1.4	Gravel/Ignimbrite	NIA
Mohale[a]	Lesotho	2006	145	3.36	600	3.52	NIA	1.4	1.4	Basalt	NIA
Segredo[a]	Brazil	1992	145	2.22	720	4.08	NIA	1.4	1.3	Basalt	NIA
Barra Grande[a]	Brazil	2005	185	3.23	666	4.17	42	1.3	1.2	Basalt	NIA
Tianshenqiao-1[a]	China	1999	178	4.25	1137	5.68	60	1.4	1.25	Limestone/Mudstone	NIA
Foz do Areia[a]	Brazil	1980	160	2.62	828	5.69	NIA	1.4	1.4	Basalt	NIA
Xingo[a]	Brazil	1994	150	3.55	850	6.89	50	1.4	1.3	Gneiss	NIA
Bakun[a]	Malaysia	2008	205	2.67	750	3.02	60	1.4	1.4	Greywacke/shale/mudstone	NIA
Nam Ngum 2[b]	Laos	2011	182	1.82	500	3.07	38	1.4	1.4	Sandstone/siltstone	12–80[b]
Miaojiaba[c]	China	2011	111	0.91	349	3.50	47	1.4	1.35	Gravel/metamorphic tuff	35[i]
Jishixia[d]	China	2007	101	0.48	300	3.25	50	1.5	1.4	Conglomerate/sandstone/mudstone	38[d]
Malutang II[e]	China	2009	154	0.12	493	2.14	48	1.4	1.3	NIA	200[e]
Cokal[f]	Turkey	NIA	83	0.35	605	4.50	62	1.4	1.4	NIA	30[f]
Zipingpu[g]	China	2006	156	0.70	664	5.20	52	1.4	1.5	NIA	175[g]
Karahnjukar[h]	Iceland	2007	196	1.53	700	4.32	60	1.3	1.25	Basalt	NIA
Machadinho[a]	Brazil	2002	127	1.60	700	4.77	55	1.3	1.2	Basalt	NIA
Itá[a]	Brazil	1999	125	2.05	881	7.04	65	1.3	1.2	Basalt	NIA
Khao laem[a]	Thailand	1984	113	1.37	910	11.00	67	1.4	1.4	Limestone	NIA
Mackintosh[a]	Australia	1981	75	0.48	465	4.96	63	1.4	1.4	Greywick	NIA

H dam height, δ dam settlement at the end of construction stage, L_c dam crest length, SF dam valley shape factor, β_{avg} average dam abutment slope, d dam slope, US-DS upstream-downstream, E_{50}^{ref} rockfill stiffness obtained from triaxial test, NIA No Information Available.

[a] [22].
[b] [23].
[c] [24].
[d] [25].
[e] [26].
[f] [27].
[g] [28].
[h] [4].
[i] [29].

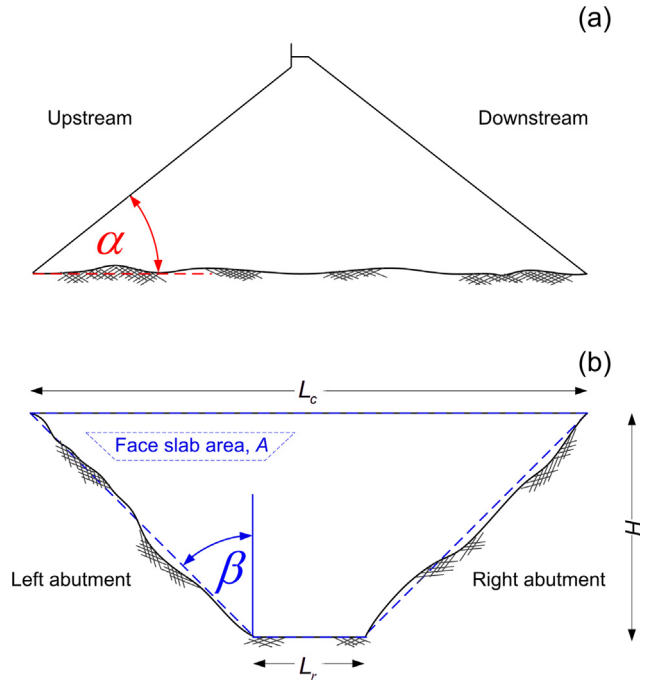

Fig. 2. (a) Typical dam section (b) Longitudinal dam cross section and lay parameters.

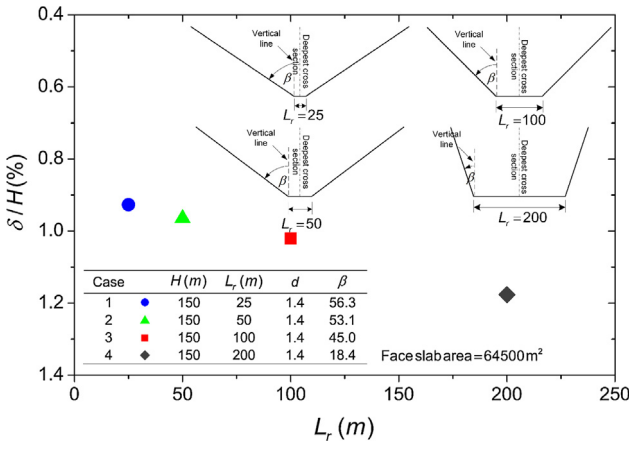

Fig. 3. comparison of δ/H for the constant face slab A.

slopes is greater than that of dams with gentler slopes. Because the computed results were obtained from cases with the same valley shape factor ($A/H^2 = 2.87$) whose A and H values are identical, the use of the parameter A/H^2 for characterizing the dam deformation covering a wide range of dam geometries is unsatisfactory. The influence of the valley shape cannot be sufficiently reflected.

Table 2
General characteristic of the dam.

Characteristics	Values	Unit
Dam height	182	m
Crest elevation	381.00	m.asl.
Crest length	500	m
Crest width	9	m
Dam volume	9.7	million m^3
Concrete face slab area	88,000	m^2
Reservoir volume	4900	million m^3

3. Analysis procedure

3.1. Finite element mesh and boundary conditions

Before performing several numerical parametric analyses, the Nam Ngum 2 (NN2) CFRD was adopted as the reference case to assess the reliability of the analysis procedure used in the study. The NN2 project is located on the Nam Ngum River in the Lao People's Democratic Republic. Dam design and construction followed the guidelines of the International Commission on Large Dams [50]. The dam was constructed using the modern compaction technique, and a comprehensive testing program was performed for the rockfill materials used. Moreover, extensive dam monitoring instruments have been deployed. The main characteristics of the NN2 CFRD are listed in Table 2.

The three-dimensional (3D) finite element analyses were performed using the ABAQUS (2016) software. Fig. 4(a) and (b) show the 3D mesh of the dam body and the rock foundation used in the analyses. In Fig. 4(a), only the left part of the model (from the left boundary to the deepest dam cross section) is depicted to show the rockfill zones and main construction stage. Four-node tetrahedral elements were used to model the dam body and rock foundation/abutment. The dam body was built of compacted rockfill materials and a concrete face slab on the side toward the reservoir. Further details about rockfill materials and construction sequences can be found in Sukkarak et al. [23]. In the analyzed case, the thickness of the embankment layer was limited to approximately 10 m at each step. Displacements at the bottom and outer sides of the rock foundation/abutment were not allowed. The concrete face slab component was modeled by 3D shell elements. The thicknesses of the shell elements varied from 0.30 m at the dam crest to 0.843 m at the toe.

The interaction behaviors at the interface between the rockfill and face slab are considered in terms of both tangent and normal directions. The sticking condition is assumed for initial condition, both of normal and tangential directions. For the behavior in normal direction, it is treated to be opened under tension and no overlapping is allowed under compression. If the shear stress in tangential direction of the interface exceeds the Mohr-Coulomb shear strength of the interface, sliding between the two surfaces occurs and no cohesion is assumed for post-slip behavior. More details can be seen in Tunsakul et al. [51]. In this study, the friction angle was 40° corresponding to the experimental work of Zhang and Zhang [52]. The cohesion parameter of 0.5 MPa was assumed. For the area of contact between the dam body and abutment/foundation, the perfect bonding (no slip condition) is defined.

3.2. Constitutive model and model parameters

The modified hardening soil (MHS) model originally developed by Schanz et al. [53] and later modified by Sukkarak et al. [23] is adopted to characterize the stress-strain response of rockfill materials. The model includes double yield functions, volumetric and shear hardening, stress-dependent stiffness and dilation behavior, which are considered to be sufficient for deformation analysis of rockfill dam under construction and first impoundment. More details are provided in Sukkarak et al. [23]. The model consists of three failure parameters according to the Mohr-Coulomb criterion, and the values of c, φ and $\Delta\varphi$ can be obtained from the relationship between the deviator stress q and the effective mean stress p'. To account for the stiffness dependence, the triaxial test stiffness input parameters for the reference (E_{50}^{ref}) can be determined from the y intercept in $\log(\sigma_3/p^{ref})$ and $\log(E_{50})$ space. Here, the slope of the trend line of this relationship is the stress-dependence parameter of the stiffness (m). In this study, $p^{ref} = 100$ kPa is chosen. Likewise, the reference of oedometer test stiffness (E_{oed}^{ref}) can be determined from the y intercept in $\log(\sigma_1/p^{ref})$ and $\log(E_{oed})$ space. Then, the slope of the trend line of this relationship is the stress-dependence parameter of the stiffness (n). The reference stiffness for elastic unloading/reloading E_{ur}^{ref} is generally set to $3E_{50}^{ref}$. For advance parameters, υ_{ur} is set to approximately 0.3. The value of K_0^{NC} can be obtained from Jacky's formula, $K_0^{NC} = 1 - \sin\varphi$. The failure ratio ($R_f$) should be smaller than 1. The overconsolidation ratio (OCR) is set equal to 1. Table 3 lists the material parameters used in this study. Fig. 5(a) and (b) show the comparison between the test data and predicted results. The modified model is capable of predicting the stress-strain-volumetric strain response of the test data. The rock foundation and abutment are assumed to be linearly elastic, with a Young's modulus of 5.0 GPa and a Poisson's ratio of 0.2.

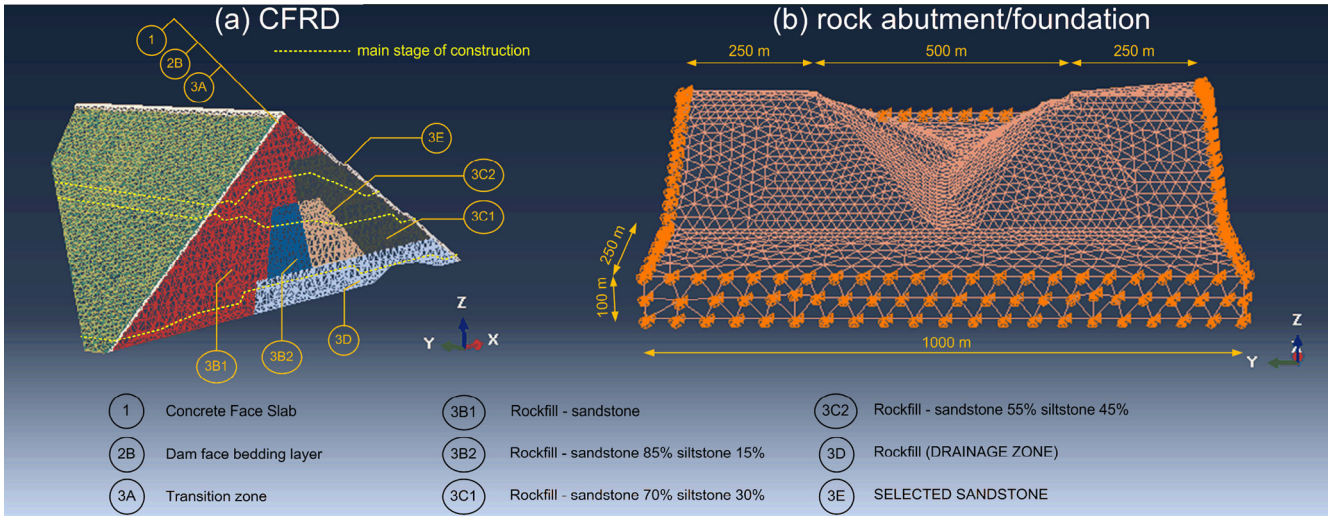

Fig. 4. Three-dimensional finite element mesh (a) CFRD (b) rock abutment/foundation.

Table 3
Model parameters for Nam Ngum 2 rockfill materials.

Parameter	Zone					
	2B	3A	3B1&3D	3B2	3C1&3E	3C2
φ_0 (°)	43.23	46.08	47.09	42.60	42	43.30
$\Delta\varphi$	1.16	2.59	2.99	2.55	2.45	3.95
ψ_0 (°)	3.2	3.2	3.2	0.5	−5	−5
E_{50}^{ref} (MPa)	65	65	80	32	20	12
E_{oed}^{ref} (MPa)	50	52	55	24	17	10
m	0.45	0.34	0.29	0.69	0.68	0.70
n	0.25	0.24	0.14	0.42	0.32	0.26
R_f	0.74	0.75	0.78	0.82	0.68	0.65
Other	$E_{ur}^{ref} = 3E_{50}^{ref}$, $p^{ref} = 100$ kPa, $c = 1$ kPa, $OCR = 1$, $K_0^{NC} = 1 - \sin\varphi$, $\upsilon_{ur} = 0.3$					

3.3. Comparison of monitoring data and computed results

Fig. 6(a) and (b) show contour plots of the dam settlement and horizontal displacement. A high concentration of settlement occurs at approximately 2/3 of the dam height in the downstream direction, as shown by blue shades. The highest settlement value is 1.587 m, which is approximately 1% of the dam height. The maximum values of horizontal displacement are 0.286 and 1.071 m for the upstream and downstream sides, respectively.

Fig. 7(a)–(f) display the layout of dam instruments for the reference case and comparisons between the computed and monitored dam deformation. Hydrostatic settlement cells (HSC) and settlement gauges (SG) were used to measure the settlement of the internal dam body, while the horizontal displacement was recorded by probe inclinometers (PI). Each instrument began to record after installation except for the PIs, which were set to zero when the dam embankment level rose to 140 m. The calculated deformation pattern is approximately the same as the monitoring data. Although the magnitudes of the computed results are generally smaller than the dam monitoring data, a good agreement can be obtained. The total strain of not larger than 5% can be found for this case. The small underprediction may be attributed to the creep behavior of the rockfill materials and to scaling effects, which have not yet been taken into consideration in this study. Further discussion of these topics can be found in Pramthawee et al. [44,54] and Sukkarak et al. [23], respectively. Based on the monitoring data, the ratio of the maximum settlement to dam height is 1.04%, which is very close to that of the dams having similar heights, i.e., Pubugou (186 m) and Maoergai (146 m). For NN2 dam, the settlement is larger at weak rockfill zone (3C1 and 3C2) toward downstream side. The deformation of this zone thus has an insignificant effect on the deformation of concrete face slab and the settlement of dam crest. The analysis method, modeling and sets of parameters used are considered suitable for further numerical investigation.

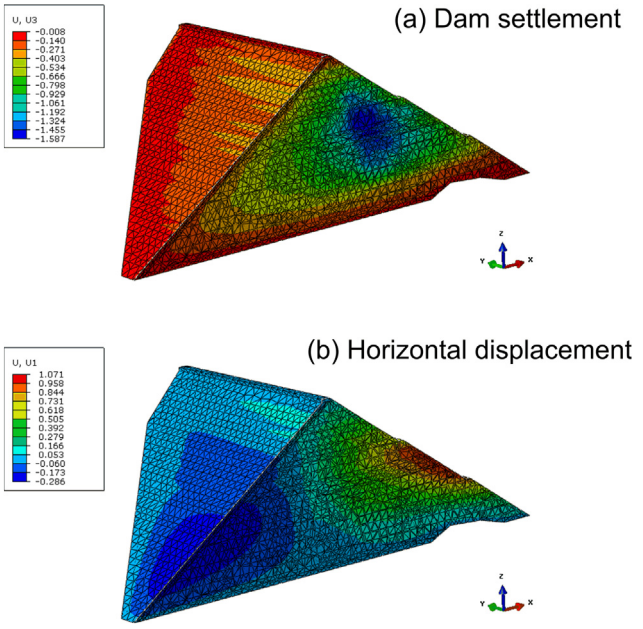

Fig. 6. Contours of the predicted results (a) Settlement (b) Horizontal displacement.

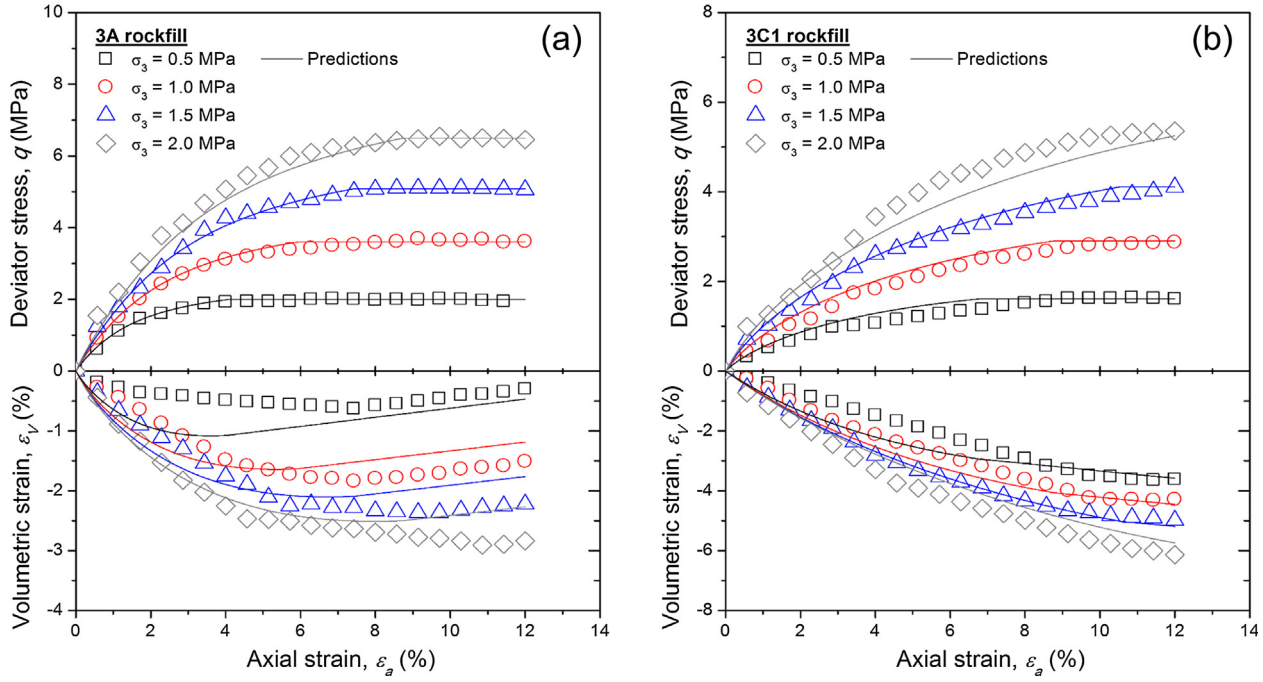

Fig. 5. (a) and (b) Comparison between the model prediction and triaxial test results of Nam Ngum 2 rockfill materials.

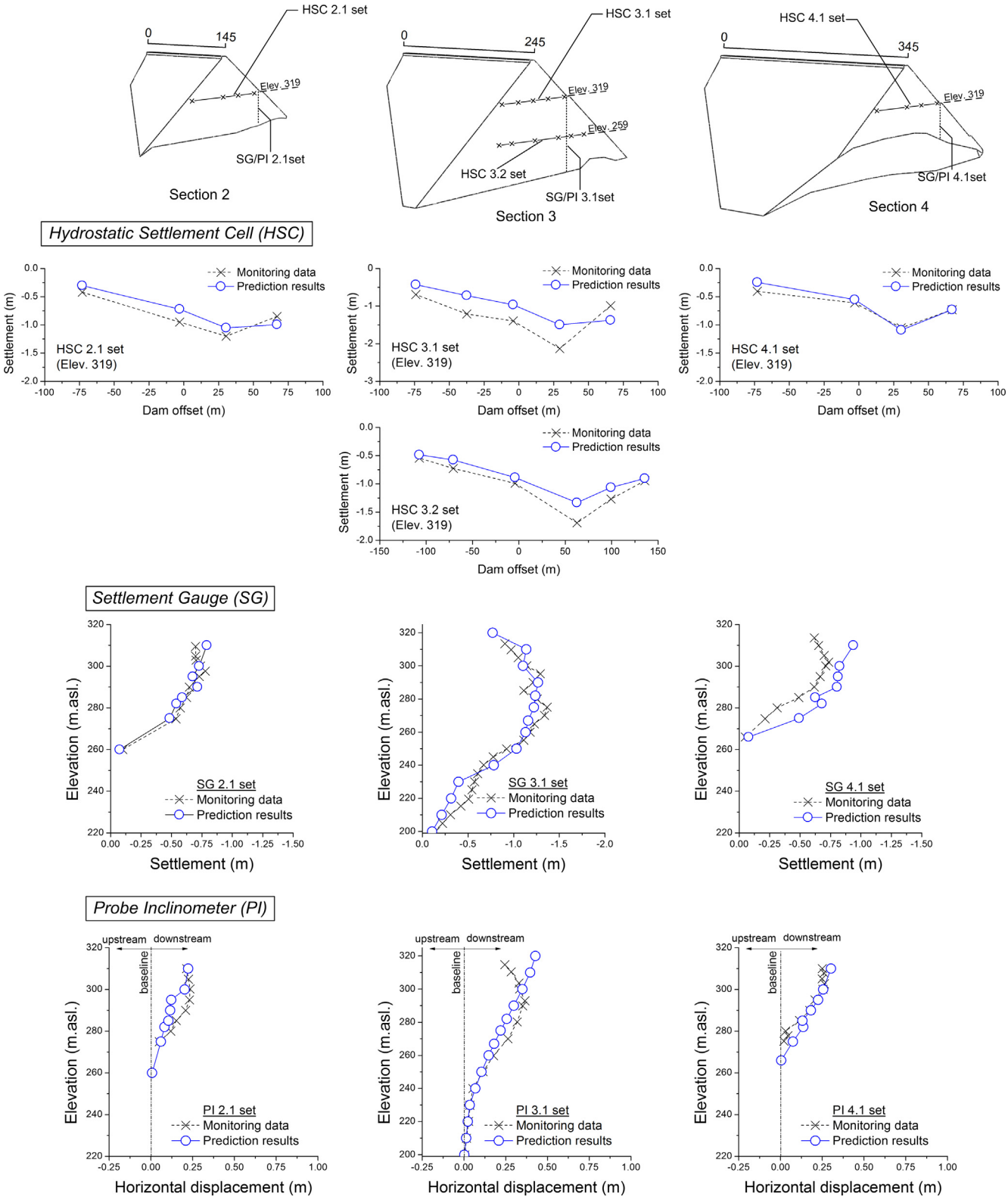

Fig. 7. Comparison between the predicted results and dam monitoring data at the end of construction stage.

4. Parametric study

4.1. Numerical assumptions and simplifications

In addition to the dam geometry and rockfill types, many other factors influence the deformation of rockfill dams, e.g., rockfill materials and their zoning, compaction [55] and construction methods. There are also several factors influencing the prediction of dam deformation by FEM, e.g., meshing and element sizes and modeling for construction sequences. It is thus difficult to take all factors into consideration in parametric studies. While the influence of type of rock fill material and the compaction method can be reflected in the rock fill

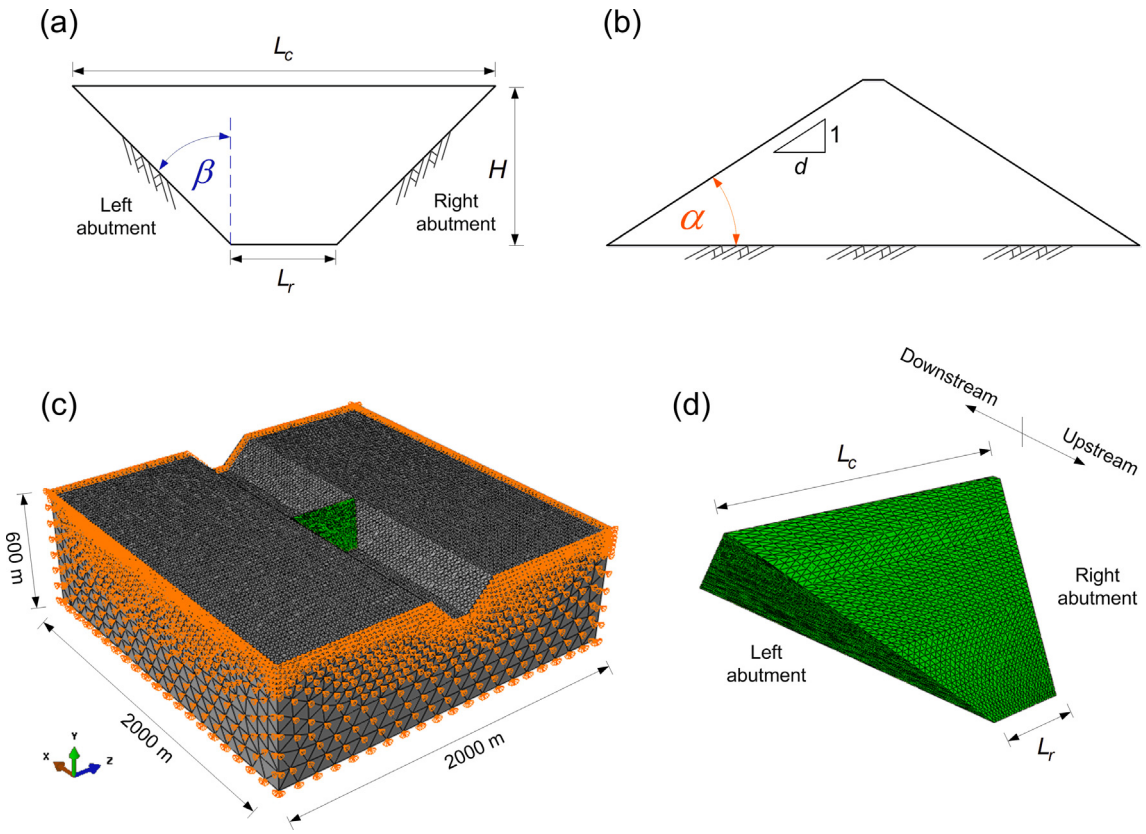

Fig. 8. (a) Representative longitudinal cross section (b) Representative typical cross section (c) and (d) 3D FE mesh of parametric analyses.

modulus value, the zoning and construction method cannot directly be represented by a simple parameter. For simplicity, the material zone has been assumed to be a homogeneous dam with the properties of rockfill used in the main zone (3C1) of the case study (E_{50}^{ref} = 20,000 kPa). The construction stage was performed with a thickness of 10 m for each layer. In the analysis, each layer was completely constructed before the construction of the above layer. The 4-node tetrahedral elements were used to model the dam body and rock foundation/abutment. The rock abutment/foundation was assumed to be sufficiently stiff with a Young's modulus of 5.0 GPa and a Poisson's ratio of 0.2. The size of the FE mesh was 2000 × 2000 × 600 m (long × width × height). The modeled dam has sufficient distance away from edge of boundary conditions. Our preliminary analysis indicated that insignificant differences of dam deformation can be obtained even the concrete face slab is not modeled. The concrete face slab component was not included in the parametric analyses. Only the end of the construction stage was of interest in the current analysis; consequently, the dam settlement in all analyses was the final settlement after construction and was obtained from the cross section at the mid-length in the longitudinal direction.

To better understand the influence of dam geometry on dam deformation behavior, this section covers a parametric study of different parameters. These include (i) abutment slope (β); (ii) crest length (L_c); (iii) river width (L_r); (iv) dam slope (d); (v) dam height (H) and (vi) rockfill stiffness (E_{50}^{ref}) (see Fig. 8(a)–(d)). A general view of the FE model for rockfill dams and the boundary conditions is shown in Fig. 8(c). In this study, a large number of 3D FE meshes have to be prepared to cover various dam geometries. The Macro Manager was utilized to record a sequence of generated ABAQUS scripting interface commands in a macro file to accommodate the preparation of FE meshes. Because this feature was used, the rock abutment (the long abutment along the riverbed in this study) was different from the real situation. However, our preliminary analysis revealed that the length of the abutment has relatively small effects on the computed dam deformation. Table 4 presents a summary of the ranges of properties varied in this parametric analysis.

Table 4
Summary of parametric analyses.

Parameter	Value	Unit
Crest length and riverbed width (L_c and L_r)	25–1000	m
Abutment slope (β)	15–75	°
Dam slope (d)	1.2, 1.4, 1.6	
Dam height (H)	100, 150, 200, 250	m
Rockfill stiffness (E_{50}^{ref})	12, 20, 80	MPa

Regarding the properties of rockfill material, in the literature, [8,22] the relationships between settlement of CFRD with various types of rockfill material were reported. It indicated that rockfill properties have the potential to be a significant contributor to the dam settlement behavior. The unconfined compressive strength (UCS) range of rockfill materials 6–240 MPa is presented in previous case studies [8]. Although the UCS value was relatively simpler, the application used was possible only with the simplified method. On the other hand, by using the current analysis method with MHS model, the stiffness parameters (E_{50}^{ref}, E_{oed}^{ref}, E_{ur}^{ref}) were required using conventional triaxial test. The E_{50}^{ref} as the main parameter in the soil model used in this study is chosen to represent the modulus of rockfill materials. The ratios of $E_{oed}^{ref}/E_{50}^{ref}$ and $E_{ur}^{ref}/E_{50}^{ref}$ were held constant at 0.85 and 3, respectively, as recommended by Sukkarak et al. [23]. The parameter is essentially obtained from triaxial tests, which are generally performed for modern dam construction. Noted that the modulus E_{50}^{ref} is different from the dam deformation modulus (E_{rc}) which is back-calculated from the measured settlement (e.g., [8,19]) as mentioned in the introduction part.

Although several aspects were carefully taken in the modeling and analysis in this study, some considerations particularly those regarding

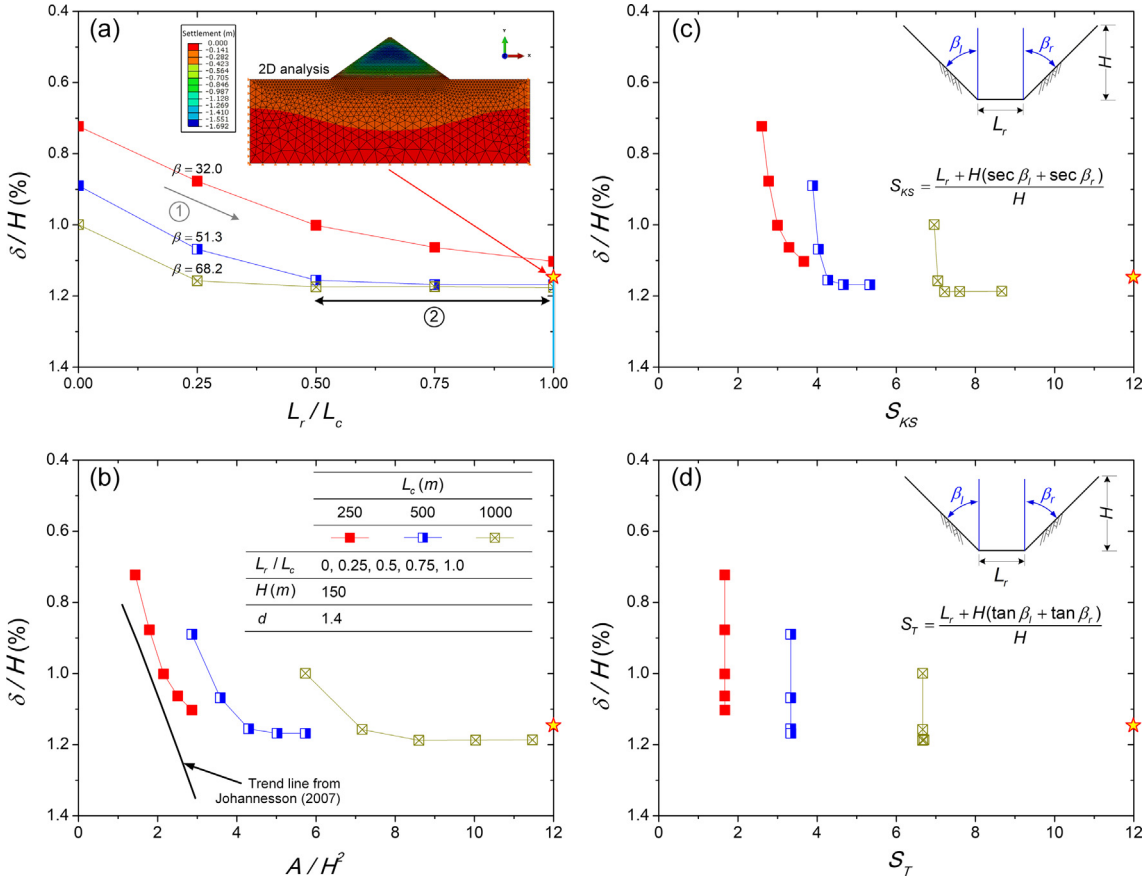

Fig. 9. Variation of dam settlement with (a) L_r/L_c (b) A/H^2 (c) S_{KS} (d) S_T.

the construction details could not be completely covered. This could slightly influence the numerical performance. However, the conclusions derived from the study were not affected by these simplifications.

4.2. Influence of abutment slope (β) and development of valley shape factor (S_β)

As discussed previously in Section 2, the values of abutment slope (β), crest length (L_c) and river width (L_r) may have significant impacts on the dam settlement behavior. A parametric study is first performed by varying L_c and L_r. The 15 analysis cases were carried out as follows: L_c = 250, 500 and 1000 m, L_r/L_c = 0, 0.25, 0.5, 0.75 and 1. The values for H of 150 m and d of 1.4 are held constant. From Fig. 9(a), the settlement (δ) behaviors affected by the variations in L_c and L_r are noticed as follows:

1. The settlement (δ) increases as L_c and L_r/L_c increase. The increases in δ/H with an increase in L_r/L_c for cases with L_c = 250 m are more pronounced than those for cases with L_c = 500 and 1000 m. The ratio δ/H increases from 0.723 when L_r/L_c = 0 to 1.103 when L_r/L_c = 1 (increased by 52.44%). The ratio δ/H increases from 0.999 when L_r/L_c = 0 to only 1.176 for L_r/L_c = 1 (increased by 17.68%) for cases with L_c = 1000 m.
2. Fig. 9(a) also shows that there is a very negligible difference in δ/H when L_r/L_c is sufficiently great (greater than 0.5 when L_c = 1000 m and 0.75 when L_c = 500 m in this study) due to the peak settlement value. Careful observation reveals that the dam abutment slope does not have a significant effect on the dam settlement (the maximum value that occurs at the mid-length) when L_r is greater than 375 m (L_r/H = 2.5) or for a canyon with a wide riverbed. In the figure, the result of two-dimensional (2D) FE analysis was also included for comparison. The FE mesh used for 2D analysis is depicted in the figure as well. The result indicated that the 3D effect of valley shape diminishes with sufficiently long dam crest and riverbed. The interest is given to cases with L_c = 250 m or with L_r/L_c of less than 0.5 whose settlement does not reach the peak value due to the existence of a valley shape effect, which is more common in engineering practice.

The computed results for δ/H are replotted against the parameter A/H^2 in Fig. 9(b) to highlight the deficiency of A/H^2 in reflecting the valley shape effect on the estimation of dam settlement. The trend line provided by Johannesson [21], as previously shown in Fig. 1, is also included in the figure. The computed results appear to be distributed in a relatively broad range. Only the computed settlements of cases with narrow valleys are seen to lie close to the trend line (linear relation). As the dam crest becomes longer (wider valley) and A/H^2 becomes larger, the differences between the computed settlements and predictions by the trend line increase. This result confirms that the parameter A/H^2 is limited in applicability to dams in narrow valleys. This result also implies that the proper relationship between dam settlement and A/H^2 is not linear. This effect is consistent with Pinto and Marques [17], who mentioned that the influence of valley shape conditions would diminish as the valley became wider. However, dam construction in open valleys or valleys with gentle slopes has increased over the past two decades, for instance, the Zipingpu, Karahnjukar, Barra Grande and Machadinho CFRDs.

The same set of analysis results were also plotted against the valley shape factors proposed by Kirn and Sarkaria [14] (S_{KS}) and Thomas [15] (S_T) as shown in Fig. 9(c) and (d), respectively. Note that the dam abutment slope has been already included in both shape factors. A considerable scatter in the data can be seen for both figures,

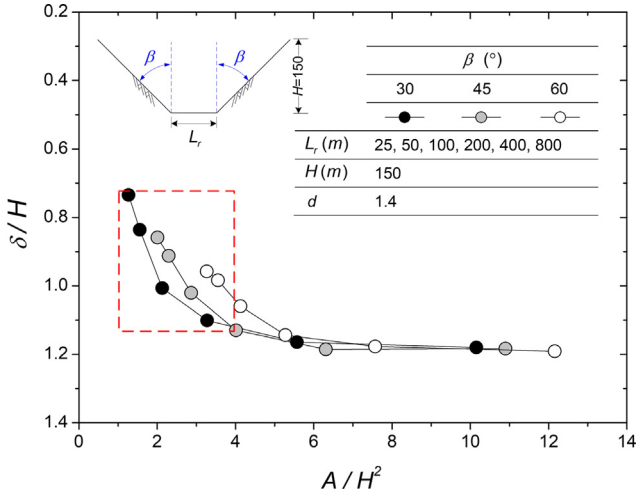

Fig. 10. Influence of dam abutment slope β on settlement.

particularly the plot with S_T. This implies that the basic parameters (ratio between L_c or L_r and H) in the development of those two shape factors could not effectively represent the valley effect.

Further investigation on the influence of the dam abutment slope (β) on the settlement of rockfill dams is performed with FE analyses of 18 cases by varying the dam lengths while controlling β from 30 to 45 and 60. The constant parameters are $H = 150$ m and $d = 1.4$. The ratio A/H^2 is employed to take into account the valley shape effect in the presentation of the results, as shown in Fig. 10. The settlement increases as A/H^2 increases before converging to a specific value regardless of the abutment slope. No significant change in settlement is observed when the A/H^2 value is greater than 6 in this study (probably for 150 m-high dams considered in this part). However, for A/H^2 in the range of 1.5–4, the settlements of dams with different abutment slopes (β) are different, although the dams possess the same A/H^2. In addition, the difference becomes larger with smaller A/H^2. As the dam abutment slope increases, the dam settlement decreases, as shown in the dashed red box. The dependence on the dam abutment slope is very obvious, particularly in the range of small A/H^2 or narrow valley conditions. This result indicates that the currently used valley shape factor (A/H^2) should be modified by taking into account the dam abutment slope.

To gain insight into the influence of the dam abutment slope on the dam vertical stress distribution, which in turn affects dam settlement, Fig. 11(a) and (b) show plots of the stress ratio ($\sigma_v/\gamma H$) along the dam height (H) at the centerline of the section at mid-length. The value of σ_v is the induced vertical stress, and γH is the calculated vertical stress using the rockfill unit weight and the considered depth from the dam crest level. The stress ratio should be unity if the vertical stress is fully transmitted from the upper layer to the considered depth, indicating the absence of an abutment slope effect. In contrast, the smaller the value is (less than unity), the more pronounced the effect of the abutment slope. In the figure, the contour plots of the distribution of the stress ratio in the dam body (on the center plane along the longitudinal direction) are also included. Fig. 11(a) depicts a comparison of cases with fixed A and H for various β (as well as L_c and L_r) whose settlement was previously shown in Fig. 3, whereas a comparison among cases with fixed L_r (only 50 m) and H for various β (as well as L_c and A) whose settlement was previously shown in Fig. 10 is illustrated in Fig. 11(b). Fig. 11(a) shows that for cases with L_c in the range of 250–1000 m, the stress ratios along the dam height (at mid-length) for cases with narrower riverbeds and gentler abutment slopes are smaller than those for cases with wider riverbeds and steeper abutment slopes. This result is attributed to the influence of abutments on vertical stress transfer; as seen in the contour figures, the blue shade (smallest stress ratio) is more concentrated in the lower part of the case with the narrowest riverbed and most gentle

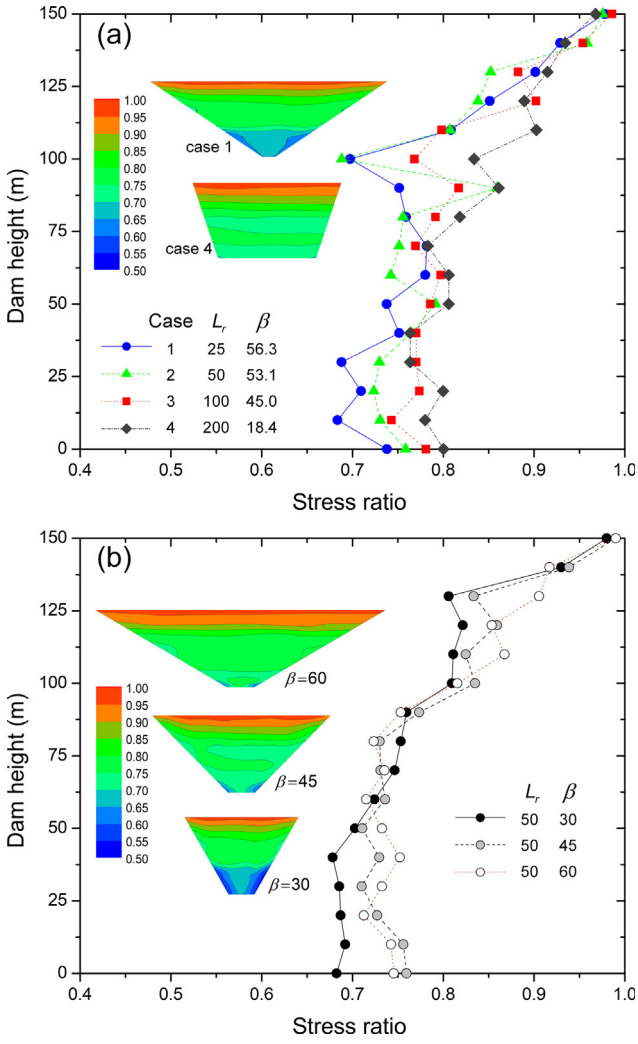

Fig. 11. Distribution of stress ratio versus dam height (a) with constant A/H^2 (b) with the influence of dam abutment slope β.

abutment slope compared to the others. However, for cases with the same riverbed width (L_r), as shown in Fig. 11(b), the blue shade becomes concentrated in the lower part of the case with the steepest abutment slope. This relation explains the mechanisms behind settlement development. With smaller stress transfer to the dam base, smaller dam settlement is thus induced. The pattern of variation of the stress ratio value is found to be consistent with the analysis presented in Giudici et al. [18]. In Giudici et al. [18], a lower stress ratio occurs at the lower part of the dam.

The numerical investigation above indicates that the currently employed valley shape factor A/H^2 is insufficient and that the linear relationship becomes unsuitable to reasonably estimate dam settlement considering a wide range of valley shapes. In this section, the valley shape factor is first modified to account for the dam abutment slope β. The modified valley shape factor S_β is a function of A/H^2 and β as expressed by:

$$S_\beta = \frac{A}{H^2} \cdot \frac{1}{\sqrt{\tan\beta}} \tag{2}$$

Fig. 12 shows the relationship between δ/H and S_β. The δ/H data that appear in the figure include those illustrated in Figs. 9 and 10 for various dam geometries or valley shapes. As shown in the figure, for a specific dam height and transverse cross section, the data for all cases from varying both river width and abutment slope for various crest lengths can reasonably be captured by using the modified valley shape

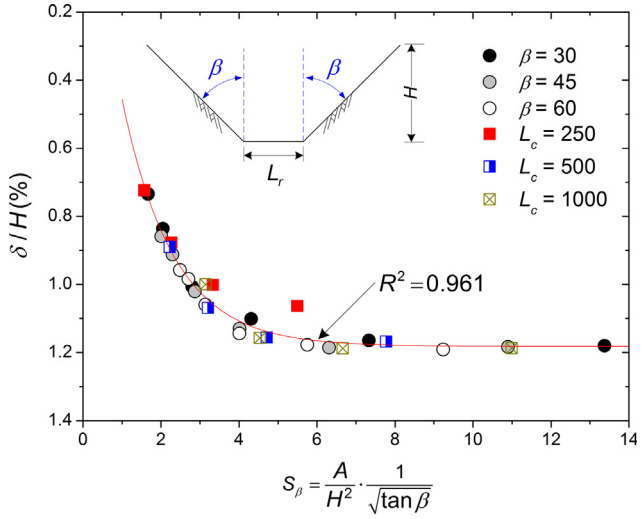

Fig. 12. Plot of δ/H and S_β.

factor S_β. An obvious rapid increase in the settlement is observed for S_β in the range of less than 3, indicating narrow valley conditions. For $S_\beta > 7$, δ/H appears to slightly increase with an increase in S_β, representing the wide valley shape for which the effect of valley shape is not crucial. The analysis can be simplified as a 2D plane strain problem.

However, in reality, the dam abutment slopes on both sides are normally not identical or asymmetrical. Song et al. [13] reported the variations in valley terrain based on data for high CFRDs in China. The abutment slope varies from 15 to 80°. Only a few dams reported are built in symmetric valleys. To further study the β effect, FE simulations were carried out with both symmetrical conditions ($\beta_l = \beta_r = \beta_{avg}$) and asymmetrical conditions ($\beta_l \neq \beta_r$). Here, β_l, β_r and β_{avg} are the left, right and average abutment slopes, respectively. Fig. 13 shows a plot of δ/H with increasing β_{avg}. The solid symbols represent the computed settlement results using $\beta_l = \beta_r$, while the cross symbols represent the results for asymmetrical conditions. As shown in Fig. 13, the computed settlements under both symmetrical and asymmetrical conditions fall in a linear relationship with β_{avg} for all cases. Thus, β_{avg} is sufficient to be used in the dam deformation estimation for unsymmetrical abutment slopes.

4.3. Influence of dam slope (d)

In the previous section, the investigation of dam geometry (which is

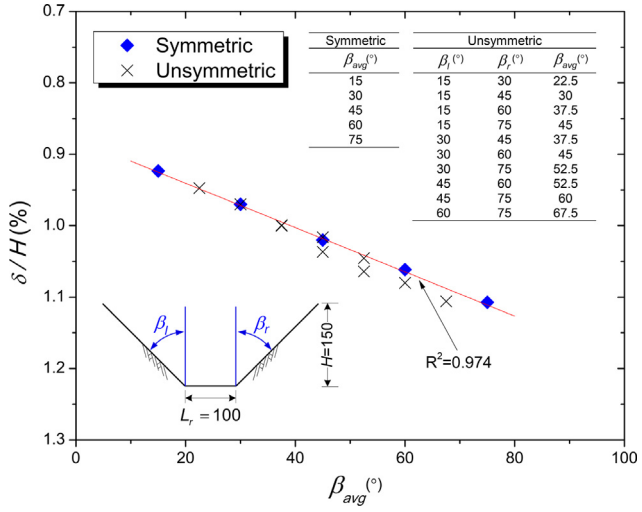

Fig. 13. Plot of δ/H and β_{avg}.

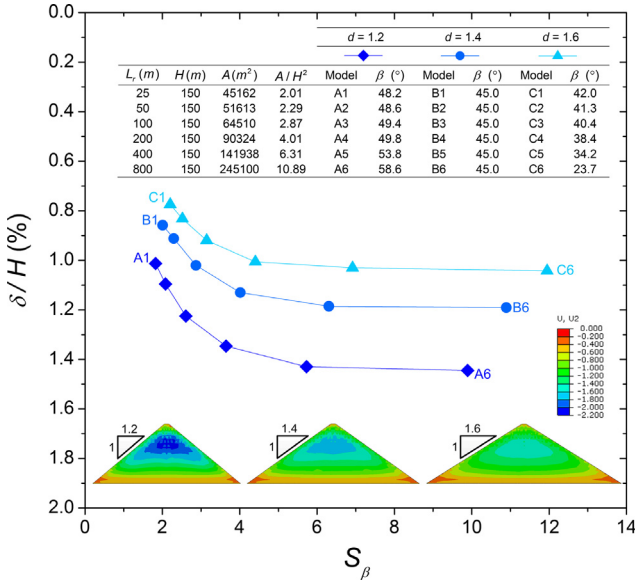

Fig. 14. Effect of dam slope (d) on the dam settlement.

essentially 3D) on settlement is mainly focused on the dam longitudinal direction, whereas the transverse cross section of the dam is fixed. In this section, the study is extended to evaluate the influence of dam slope on deformation behavior by analyzing an additional 18 cases. The dam slope is denoted by d values that vary between 1.2 and 1.6 instead of by an angle. This range was selected in accordance with one observed in the typical dam design. The dam settlement is plotted against S_β for various d, as shown in Fig. 14. The computed settlements appear to increase significantly with decreasing d. The dam settlement behavior is found to depend not only on the abutment slope β but also on the dam slope d. However, it seems that d affects only the magnitude of settlement, and the variations with S_β for different d are practically similar. This result implies that it is unnecessary to take the parameter d into account for the valley effect; the parameter S_β is sufficient to quantify the valley effect. Contour plots of the computed settlements of 3 analysis cases (cases A6, B6 and C6 with d = 1.2, 1.4 and 1.6, respectively) with the same dam length are also included in the figure. The maximum settlement (U2) is shaded dark blue. Although the magnitudes are different, a similar distribution pattern of the contour plots is obtained.

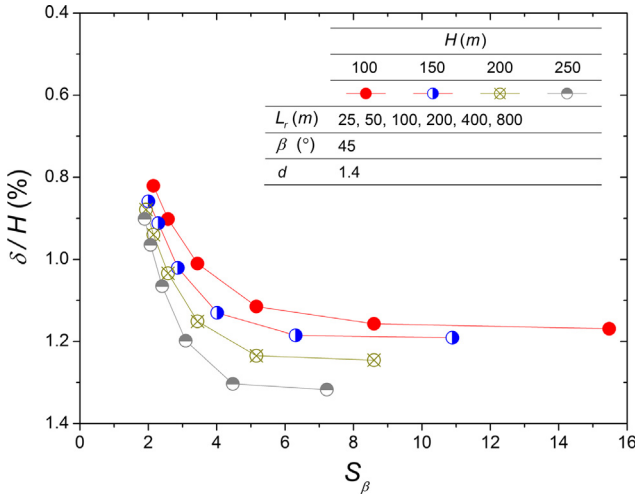

Fig. 15. Effect of dam height (H) on the dam settlement.

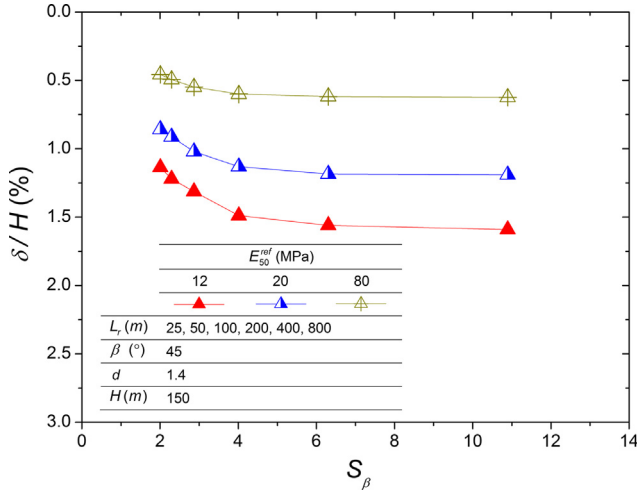

Fig. 16. Effect of rockfill stiffness (E_{50}^{ref}) on the dam settlement.

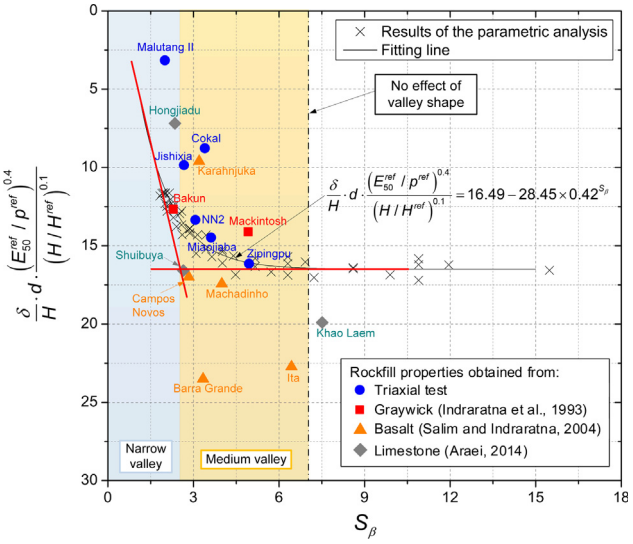

Fig. 17. Comparison of the 3D FE results with case histories.

4.4. Influence of dam height (H)

In the present study, the influence of the dam height (H) was studied by varying H, and 18 analysis cases were performed in which H was varied between 100 and 250 m with L_r = 25–800 m. The constant parameters are β = 45 m and d = 1.4 following common practice. Fig. 15 shows the calculated dam settlements based on the modified valley shape factor S_β. It is shown that each dam height exhibits a similar development tendency but different magnitude. With increases in H and S_β, the settlement ratio (δ/H) increases before approaching the maximum δ/H at a certain value of S_β. It is interesting to note that the maximum δ does not linearly increase with H, indicating the nonlinear behavior of rockfills. The influence of S_β does not seem to affect the computed results when $S_\beta > 7$.

4.5. Influence of rockfill stiffness

In the present study, the influence of the rockfill modulus was investigated by conducting numerical analyses with different moduli (E_{50}^{ref}) for the rockfill material. Eighteen cases for which E_{50}^{ref} was varied between 12 and 80 MPa were carried out. Fig. 16 shows the relations of δ/H and S_β for the computed results corresponding to different E_{50}^{ref} values. It is clear that the dam settlement decreases with increasing modulus parameters. This result is consistent with a previous study by Xing et al. [56] using other soil models. Overall, the distribution pattern of dam settlement is similar to that from a previous study. The value of E_{50}^{ref} solely influences the magnitude of settlement, and the variations with S_β for different E_{50}^{ref} are practically similar. However, the influence of E_{50}^{ref} on the magnitude of settlement is greater than that of H for the ranges considered in this study.

4.6. Equation for estimating dam settlement considering the effects of dam geometry

Based on the analysis results presented thus far, the dam deformation behavior and its magnitude depend on several factors. Among the factors explored in this study, the abutment slope (β) is found to affect both the magnitude and pattern of deformation regarding the dam geometry due to the valley effect. The original valley shape factor A/H^2 is thus improved to the modified shape factor S_β. The other factors (i.e., d, H, and E_{50}^{ref}) affect only the settlement magnitude. Therefore, it is reasonable to exclude S_β from other factors in the development of a simple equation to predict dam settlement. To accomplish this purpose, a power equation has been selected for estimating dam settlement as a function of β, d, H, and E_{50}^{ref}, as shown by Eq. (3):

$$\frac{\delta}{H}\cdot d\cdot\frac{(E_{50}^{ref}/p^{ref})^{0.4}}{(H/H^{ref})^{0.1}} = a - b\times c^{S_\beta} \tag{3}$$

where the constants a, b and c are 16.49, 28.45 and 0.42, respectively, in this study, which can be obtained from regression analysis of the data. In the current study, a total of 103 numerical computations and 16 actual dam data points were collected. The value of E_{50}^{ref} was normalized by p^{ref} = 100 kPa, while the dam height was nondimensionalized by H^{ref} = 50 m. Fig. 17 shows the relationship between S_β and the proposed term. It is clearly seen that all data for dam settlement with several varied factors can be well captured by the proposed equation. The predictive ability of the equation can be further inspected by plotting the data from the dam case histories in the figure. Note that the blue circle symbols represent a total of 6 well-documented data, including the typical layout of the dam (β and d), dam instrument data, and triaxial test results. For others, which lack triaxial test data, the E_{50}^{ref} values used are collected from experimental data of the same rockfill type available in the literature. The plot indicates that the proposed equation is able to predict reasonably well, especially for the data with complete information. For data with information only on dam geometry, although some scattering is noticed, the figure shows the improvement of the prediction, particularly in the cases of Hongjiadu, Mackintosh, Karahnjuka and Machadinho (compared to Fig. 1). For dams constructed in wide valleys, better prediction is also observed, especially for Khao laem. However, data from a few cases (Ita and Barra Grande) are far from the proposed line. Note that the settlement magnitude in both cases ($\delta/H > 1.5$) is much larger than most of the dam data found in the literature (δ is found to be less than 1% of dam height) [21,22]. Based on the proposed relation in this study, for the preliminary design stage, dam engineers and designers can reasonably estimate the dam settlement.

From the relationship illustrated in the figure, it is also seen that when $S_\beta > 7$, the influence of valley shape disappears. Thus, wide valley conditions can be specified as referring to $S_\beta > 7$. For dams whose geometry falls in this range (Ita and Khao Laem dams), the proposed equation gives a more acceptable prediction than the previous one. For narrow and medium valleys, it may be distinguished by the intersection point (S_β = 2.5) between 2 secant lines, as shown in the figure.

5. Conclusion and discussion

This paper presents a series of 3D finite element analyses aiming to investigate the influence of dam geometry (abutment slope, dam slope

and dam height) and the stiffness of rockfill material on the settlement behavior of rockfill dams. The validity of the analysis method is verified with the well-instrumented case of the Nam Ngum 2 CFRD. The following findings and conclusions are reached:

- Numerical findings reveal that the valley shape has a significant influence on the dam settlement behavior. According to the investigation of the effects of L_c, L_r and β, the original valley shape factor A/H^2 is proven to be insufficient for representing the effects of dam geometry and incorporating the effects of valley shape. All computed results show that the effect of variations in β on dam settlement is more sensitive for dams with low A/H^2 values. Then, the modified valley shape factor S_β is proposed in this study to better capture the influence of dam geometry on the dam settlement behavior.
- Regarding the abutment slope, the average abutment slope β_{avg} indicates good prediction capability for asymmetrical abutment slopes.
- The modified shape factor S_β can be used as a reliable alternative to characterize the valley effect for the estimation of dam settlement. The values of 2.5 and 7 are suggested to distinguish between narrow and medium valleys and between medium and wide valleys, respectively.
- In the proposed power equation for estimating dam settlement $\frac{\delta}{H}\cdot d\cdot\frac{(E_{50}^{ref}/p^{ref})^{0.4}}{(H/H^{ref})^{0.1}} = 16.49 - 28.45\times 0.42^{S_\beta}$, the predicted lines give satisfactory results for most databases. This equation can satisfactorily characterize the settlement of dams with various geometries at the end of construction and would be useful at the preliminary design stage.

However, the obtained results are based on some simplifications in numerical method adopted in the study, particularly the exclusion of concrete slab and consideration of single rockfill type. Besides, the impoundment stage was not taken into account. Broader set of numerical analyses are needed to enhance the findings from this study.

Acknowledgments

The authors gratefully acknowledge the financial support from King Mongkut's University of Technology Thonburi (KMUTT) under Research Grant No. CE-KMUTT 6204. They are also indebted to the CK Power Public Company Limited and Nam Ngum 2 Power Company Limited for providing the valuable data.

References

[1] Zhang G, Zhang JM. Modeling of low-cement extruded curb of concrete-faced rockfill dam. Can Geotech J 2011;48(1):89–97.
[2] Wang X, Solymár ZV. Predicting the behavior of an earth and rockfill dam under construction. Tunn Undergr Space Technol 1997;12(4):461–72.
[3] Jiang XW, Wan L, Wang XS. Estimation of fracture normal stiffness using a transmissivity-depth correlation. Int J Rock Mech Min Sci 2009;46(1):51–8.
[4] Modares M, Quiroz J. Structural analysis framework for concrete-faced rockfill dams. Int J Geomech ASCE 2016;16(1):04015024.
[5] Cooke J, Sherard J. Concrete-face rockfill dam: II. Design. J Geotechn Eng ASCE 1987;113(10):1113–32.
[6] Cooke JB. Progress in rock-fill dams: (18th Terzaghi Lecture). J Geotechn Eng ASCE 1984;110(10):1381–414.
[7] Clements R. Post-construction deformation of rockfill dams. J Geotechn Eng ASCE 1984;110(7):821–40.
[8] Hunter G, Fell R. Rockfill modulus and settlement of concrete face rock-fill dams. J Geotechn Geoenviron Eng ASCE 2003;129(10):909–17.
[9] Gurbuz A. A new approximation in determination of vertical displacement behavior of a concrete-faced rockfill dam. Environ Earth Sci 2011;64:883–92.
[10] Rezaei M, Salehi B. The effect of changing the geometry and compaction degree on arching of earth dams. Proc Geo-Front 2011:3207–16.
[11] Moradi M, Shirgir V, Ghanbari A. An approximate equation for the estimation of arching due to the shape and hardness of valley in earth dams. Electron J Geotech Eng 2014;19:6343–52.
[12] Han B, Zdravkovic L, Kontoe S, Taborda DM. Numerical investigation of the response of the Yele rockfill dam during the 2008 Wenchuan earthquake. Soil Dyn Earthquake Eng 2016;88:124–42.
[13] Song R, Chai J, Xu Z, Qin Y, Cao J. Influence of abutment slope angle variety on the deformation and stress of the concrete-faced rockfill dam during initial impoundment. Int J Civil Eng 2018:1–15. in press.
[14] Kirn ID, Sarkaria GS. Influence of canyon shape on the design of concrete dams. Civil Eng Public Works Rev 1955;50:585.
[15] Thomas HH. The engineering of large dams. New York: John Wiley and Sons Inc.; 1976.
[16] Znamensky D. Valleys shape influence on the volume safety factor and arch effect of high CFR recently built in brazil. Brasilia: Commission Internationale des Grands Barrages; 2009.
[17] Pinto NLS, Marques PL. Estimating the maximum face deflection in CFRDs. Hydropower Dams 1998;6:28.
[18] Giudici S, Herweynen R, Quinlan P. HEC experience in concrete faced rockfill dams-Past, present and future. In: Proceedings of international symposium on concrete faced rockfill dams. International committee on large dams, Beijing, ICOLD; 2000. p. 29–46.
[19] Kim Y, Kim B. Prediction of relative crest settlement of concrete-faced rockfill dams analyzed using an artificial neural network model. Comput Geotechn 2008;35(3):313–22.
[20] Pinto NLS. Very high CFRD dams-Behavior and design features. In: III Symposium on CFRD-Dams Honoring J. Barry Cooke; 2007. Florianópolis, Brazil.
[21] Johannesson P. Design improvements of high CFRDs constructed of low modulus rock. In: III Symposium on CFRD-Dams Honoring J; 2007. Barry Cooke, Florianópolis, Brazil.
[22] Cruz P, Materon B, Freitas M. Concrete face rockfill dams. Sao Paulo: CRC Press; 2010.
[23] Sukkarak R, Pramthawee P, Jongpradist P. A modified elasto-plastic model with double yield surfaces and considering particle breakage for the settlement analysis of high rockfill dams. KSCE J Civ Eng 2017;21:734–45.
[24] Feng D, Zhang G, Zhang J. Three-dimensional seismic response analysis of a concrete-faced rockfill dam on overburden layers. Front Archit Civil Eng China 2010;4(2):258–66.
[25] Zhang G, Zhang JM, Yu Y. Modeling of gravelly soil with multiple lithologic components and its application. Soils Found 2007;47(4):799–810.
[26] Jia Y, Chi S. Back-analysis of soil parameters of the Malutang II concrete face rockfill dam using parallel mutation particle swarm optimization. Comput Geotechn 2015;65:87–96.
[27] Arici Y, Özel HF. Comparison of 2D versus 3D modeling approaches for the analysis of the concrete faced rockfill Cokal Dam. Earthquake Eng Struct Dyn 2013;42:2277–95.
[28] Xu B, Zou D, Liu H. Three-dimensional simulation of the construction process of the Zipingpu concrete face rockfill dam based on a generalized plasticity model. Comput Geotechn 2012;43:143–54.
[29] Wen L, Chai J, Xu Z, Qin Y, Li Y. Monitoring and numerical analysis of behaviour of Miaojiaba concrete-face rockfill dam built on river gravel foundation in China. Comput Geotechn 2017;85:230–48.
[30] Zhu B, Rao B, Jia J, Li Y. Shape optimization of arch dams for static and dynamic loads. J Struct Eng 1992;118(11):2996–3015.
[31] Hu L, Chen F, Li Y. Research of optimal design for gravity dam based on niche genetic algorithm. CESM 2011; Part II, CCIS(176):323–328.
[32] Akbari J, Ahmadi MT, Moharrami H. Advances in concrete arch dams shape optimization. Appl Math Model 2011;35(7):3316–33.
[33] Khatibiniaa M, Khosravib Sh. A hybrid approach based on an improved gravitational search algorithm and orthogonal crossover for optimal shape design of concrete gravity dams. Appl Soft Comput 2014;16:223–33.
[34] Banerjee A, Paul DK, Acharyya A. Optimization and safety evaluation of concrete gravity dam section. KSCE J Civ Eng 2015;19(6):1612–9.
[35] Mahani AB, Shojaee S, Salajegheh E, Khatibinia M. Hybridizing two-stage metaheuristic optimization model with weighted least squares support vector machine for optimal shape of double-arch dams. Appl Soft Comput 2015;27:205–18.
[36] Özkuzukiran S, Özkan MY, Özyazicioğlu M, Yildiz GS. Settlement behaviour of a concrete faced rockfill dam. Geotech Geol Eng 2006;24:1665–78.
[37] Kim YS, Seo MW, Lee CW, Kang GC. Deformation characteristics during construction and after impoundment of the CFRD-type Daegok Dam, Korea. Eng Geol 2014;178:1–14.
[38] Mahabad NM, Imam R, Javanmardi Y, Jalali H. Three-dimensional analysis of a concrete-face rockfill dam. Proc ICE - Geotechn Eng 2014;167(4):323–43.
[39] Sukkarak R, Pramthawee P, Jongpradist P, Kongkitkul W, Jamsawang P. Deformation analysis of high CFRD considering the scaling effects. Geomech Eng 2018;14(3):211–24.
[40] Zhou W, Chang XL, Zhou CB, Liu XH. Creep analysis of high concrete-faced rockfill dam. Int J Numeric Methods Biomed Eng 2010;26:1477–92.
[41] Zhou W, Hua J, Chang X, Zhou C. Settlement analysis of the Shuibuya concrete-face rockfill dam. Comput Geotechn 2011;38(2):269–80.
[42] Zheng D, Cheng L, Bao T, Lv B. Integrated parameter inversion analysis method of a CFRD based on multi-output support vector machines and the clonal selection algorithm. Comput Geotechn 2013;47:68–77.
[43] Wei K, Zhu S. A generalized plasticity model to predict behaviors of the concrete-faced rock-fill dam under complex loading conditions. Eur J Environ Civil Eng 2013;17(7):579–97.
[44] Pramthwee P, Jongpradist P, Sukkarak R. Integration of creep into a modified hardening soil model for time-dependent analysis of a high rockfill dam. Comput Geotech 2017;91:104–16.
[45] Seo MW, Ha IS, Kim YS. Behaviour of concrete-faced rockfill dams during initial impoundment. J Geotechn Geoenviron Eng ASCE 2009;135:1070–81.

[46] Sowers GF, Williams RC, Wallace TS. Compressibility of broken rock and settlement of rockfills. In: Proc. 6th ICSMFE, Montreal, vol. 2;1965. p. 561–5.
[47] Parkin AK. The compression of rockfill. Aust Geomech J 1977;7:33–9.
[48] Soydemir C, Kjaersli B. Deformation of membrane-faced dams. Design parameters in geotechnical engineering. BGS, London 1979;3:281–4.
[49] Kermani M, Konrad JM, Smith M. An empirical method for predicting post-construction settlement of concrete face rockfill dams. Can Geotech J 2017;54(6):755–67.
[50] ICOLD. Concrete face rockfill concepts for design and construction dams, committee on materials for fill dams 2004:24–86.
[51] Tunsakul J, Jongpradist P, Kongkitkul W, Wonglert A, Youwai S. Investigation of failure behavior of continuous rock mass around cavern under high internal pressure. Tunn Undergr Space Technol 2013;34:110–23.
[52] Zhang G, Zhang JM. Unified modeling of monotonic and cyclic behavior of interface between structure and gravelly soil. Soils Found 2008;48(2):231–45.
[53] Schanz T, Vermeer PA, Bonnier PG. The hardening soil model – formulation and verification. Proceedings plaxis symposium-beyond 2000 in computational geotechnics. Amsterdam, Rotterdam: Balkema; 1999.
[54] Pramthawee P, Jongpradist P, Kongkitkul W. Evaluation of hardening soil model on numerical simulation of behaviors of high rockfill dams. Songklanakarin J Sci Technol 2011;33(3):325–34.
[55] Oldecop L, Alonso E. Theoretical investigation of the time-dependent behaviour of rockfill. Géotechnique 2007;57(3):287–301.
[56] Xing HF, Gong XN, Zhou XG, Fu HF. Construction of concrete faced rockfill dams with weak rocks. J Geotechn Geoenviron Eng ASCE 2006;132(6):778–85.